Biofidelity Improvement of Advanced Pedestrian Legform Impactor in Rebound Phase

Atsuhiro Konosu, Takahiro Isshiki, Jacobo Antona-Makoshi, Yu-ki Higuchi, Derek Winter, Yukou Takahashi

Abstract Although the advanced pedestrian legform impactor has successfully addressed a number of issues of the flexible pedestrian legform impactor, the large spring back during the rebound phase notably seen in impacts with low bonnet leading edge cars has not yet been resolved. The aim of this study was to improve the design of the advanced pedestrian legform impactor to address this issue without sacrificing its advantages. The heavier femur and the stiffer flesh of the impactor, compared to those of a human, were confirmed to be responsible for the spring back due to the accumulation and release of a large bending energy of the femur. To improve the response in the rebound phase, specifically for low bonnet leading edge cars, a bumper system was added to an advanced pedestrian legform impactor model to reduce the accumulated energy of the femur in proportion to the degree of the hip adduction angle. The validity of the system was evaluated in impact simulations with low bonnet leading edge car models. Its hardware was designed to realise predicted performance in car tests, while maintaining durability. The results of the functional tests show that the bumper design substantially reduced the spring back of the advanced pedestrian legform impactor in impacts with low bonnet leading edge cars, without sacrificing the impactor performance in impacts with higher bonnet leading edge cars.

Keywords Legform impactor, lower limb injuries, pedestrian safety.

I. INTRODUCTION

The lower limbs and the head of pedestrians are the major injured body regions in car-to-pedestrian accidents worldwide [1]. Specifically, in 2017 Japanese accident statistics, the percentage of injury to the lower limbs was the largest of all body regions in pedestrian severe injury, followed by the head, at 38.1 % and 20.5 %, respectively [2]. To reduce the number of severe lower limb injuries in car-to-pedestrian accidents, the United Nations (UN) global technical regulation for pedestrian safety [3] and the UN regulation for pedestrian safety [4] were developed by introducing the Flexible Pedestrian Legform Impactor (FlexPLI) as a test tool to evaluate pedestrian lower limb protection performance of a car.

The FlexPLI representing only the lower limb of a pedestrian possesses some limitations. First, because the FlexPLI lacks the upper body representation, it tends to be projected forward earlier than the lower limb of a human full body in high-bumper car impacts [5]. Second, the lack of the upper mass (UM) along with the rectangular shape of the knee condyles cause unrealistic longitudinal rotation of the lower limb in oblique impacts [6]. Third, as the knee of the FlexPLI is heavier than that of a human, it generates excessive bumper contact force [7]. Forth, the FlexPLI produces excessive peak values of injury measures compared to those of a human in the rebound phase, specifically in impacts with low-bonnet leading edge (BLE) cars [8].

To address these issues, the advanced Pedestrian Legform Impactor (aPLI) was introduced. To determine specifications of the aPLI by using computer aided engineering (CAE) techniques effectively, a baseline finite element (FE) model for the aPLI was developed based on the FlexPLI model (aPLI baseline FE model). First, the early forward projection of the FlexPLI in impacts with high-bumper cars was addressed by adding an optimised UM on the top of the femur via a free cylindrical hip joint [9]. Second, to achieve a biofidelic response in oblique impacts with respect to the bumper, biofidelic round shapes of the knee condyles were introduced in addition to the attached UM [10]. Third, to improve the impactor's biofidelity in terms of bumper contact forces, the mass of the knee joint was reduced by keeping the total mass of each of the thigh and the leg [10]. The effectiveness of the developed aPLI baseline FE model to mitigate the three issues (earlier forward projection, non-biofidelic longitudinal rotation in oblique impacts and larger bumper contact forces) was confirmed under

Atsuhiro Konosu (+81-29-856-0883, akonosu@jari.or.jp), Takahiro Isshiki, Jacobo Antona-Makoshi and Yu-ki Higuchi are Researchers at the Japan Automobile Research Institute, Tsukuba, Japan. Derek Winter is the ATD Engineering Manager in Cellbond, Yukou Takahashi is the Chairperson of the Pedestrian Safety Experts Group at the Japan Automobile Manufacturers Association, Inc., Tokyo, Japan.

the impact conditions with the 36 simplified car models (SCMs), which consisted of three parts (BLE, bumper, spoiler), and represented a wide range of BLE and lower bumper reference line (LBRL) heights (BLE from 650 to 1200 mm, LBRL from 215 to 615 mm) and three different impactor-to-bumper horizontal angles (0 degrees and $\pm$ 40 degrees) [10].

On the contrary, the mechanism of the excessive peak values of injury measures compared to those of a human in the rebound phase, especially in low-BLE car impacts, has not been clarified, and the aPLI baseline FE model has been evaluated against the issue by using only one single low-BLE SCM from our previous study [10].

The aim of this study was to clarify the mechanism of the excessive peak values of the aPLI in the rebound phase, specifically in impacts against low-BLE cars, and to improve the design of the aPLI to address this issue without sacrificing its advantages to the higher BLE cars.

Two-step approach was taken. First, the mechanism of the excessive peak values of the aPLI in the rebound phase was analised, clarifying that the heavier femur and the stiffer flesh of the aPLI compared to those of a human are responsible for a large femoral bending moment (BM). This accumulates large energy in the femur during the early stage of the impact. The large energy stored by the femur is then released as the femur springs back, leading to an increase of peak injury values, specifically medial collateral ligament (MCL) elongation. Second, based on the clarified mechanism, an effective measure was developed to solve the issue, and the effectiveness of the measure was evaluated by installing it in an aPLI FE model (aPLI modified FE model) and an aPLI hardware unit. The aPLI modified FE model was developed in this research based on the design details of the aPLI hardware unit to accurately represent its performance in actual car impacts because the aPLI hardware unit incorporates some design changes to the aPLI baseline FE model to enhance repeatability, reproducibility and usability.

II. METHODS

CAE Models and Software

For this study, seven real car models (RCMs) developed by car manufacturers were used to represent selected commercial cars based on CAD data. The RCMs comprised four sedans (Sedan-1 through 4), one mini van and two Sport Utility Vehicles (SUVs) (SUV-1 and 2), with BLE heights ranging from 657 mm to 947 mm (Figure 1). The detailed construction of the seven RCMs cannot be disclosed because of confidentiality reasons. The BLE height for each RCM is presented, as this information is critical for the study. Since excessive peak values of injury measures in the rebound phase are most evident in low-BLE cars, Sedan-1 with the lowest BLE was used to analyse the mechanism of the rebound response and to develop an effective measure. The other six car models were used to evaluate robustness of the effect of the measure developed for Sedan-1.

The aPLI modified FE model was developed by referring to design details of the aPLI hardware unit to accurately represent its performance (Appendix A). Specifically, the flesh of the aPLI hardware unit had been moulded to ensure repeatability, reproducibility and usability performance compared to the multi-layer neoprene sheets used for the flesh of the aPLI baseline FE model. Therefore, revision of the model was needed to capture the changes introduced at fabrication so as not to miss the potential sources of the excessive peak values of injury measures. The aPLI modified FE model was validated by comparing its response to aPLI experimental data, including quasi-static 3-point bending certification tests of the thigh, knee and leg, and dynamic full-assembly certification tests (Appendix A).

A 50th percentile adult male human body model (HBM) previously developed [11, 12, 13] was used in the current study. Its biofidelity has been validated in detail against numerous post-mortem human subject test datasets, including quasi-static and dynamic knee ligament tensile tests, dynamic 3-point bending tests (thigh, leg, femur, tibia and fibula), dynamic 4-point and 3-point knee bending tests and full-scale real-car impact tests.

All the simulations in this study were conducted with Virtual Performance Solution (VPS) by ESI group (Paris, France).

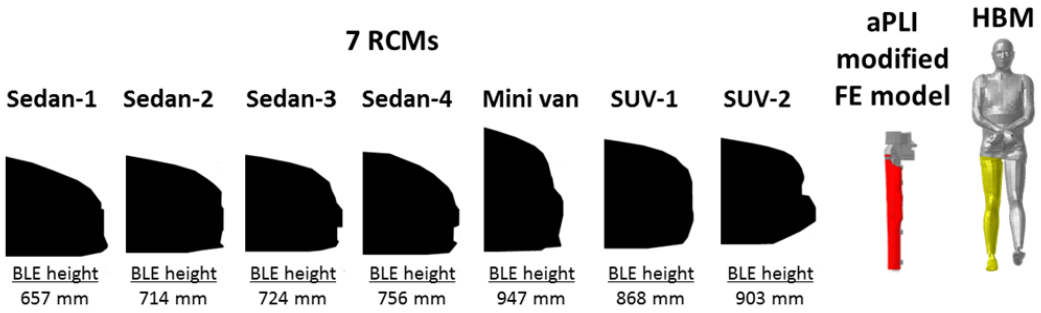

Fig. 1. Overview of CAE models used in this study.

Step 1: Analysis of Mechanism

In order to analyse the mechanism of generating the excessive peak values in low-BLE car impacts, the RCM model with the lowest BLE (Sedan-1) was applied to simulate a 40 km/h lateral impact to the aPLI modified FE model and the HBM (Figure 2). The HBM was hit laterally from the right. For these simulations, the aPLI modified FE model and the HBM were positioned 25 mm above ground level to compensate for the height of the sole of the shoe. A gravity field was applied entirely to each model. Since the excessive peak values in the rebound phase were observed in the round-robin tests using the aPLI hardware units regardless of the lateral location of bumper impacts, impacts were delivered to both the aPLI modified FE model and the HBM by the centre of the bumper of the RCM as a representative load case. The positioning of the HBM was defined with the lower limb on the struck side vertical to the ground and the non-struck side rotated 20 degrees forward about the hip joint. The contact setting between the lower limbs was not applied because its influence on the peak value of injury measures was found to be small (Appendix B) and the aPLI only mimics a single lower limb. Those settings are also used in Step 2.

The time histories of corresponding injury measures (BM at three locations along the thigh, BM at four locations along the leg and elongation of MCL) were extracted from the simulations with the aPLI modified FE model and the HBM (Appendix C), and then compared to each other and analysed. This analysis allowed hypothesising the mechanism of the excessive peak values in the rebound phase. To validate the hypothesis, a modified HBM was developed by adjusting the flesh and bone mass distributions to those of the aPLI, and by rigidising several areas of the flesh, to artificially mimic the heavier femur and the stiffer flesh of the aPLI (Figure 3). The modified HBM was subjected to the same lateral impact simulation against the RCM, and the time histories of the injury measures were compared with those of the original HBM and the aPLI modified FE model.

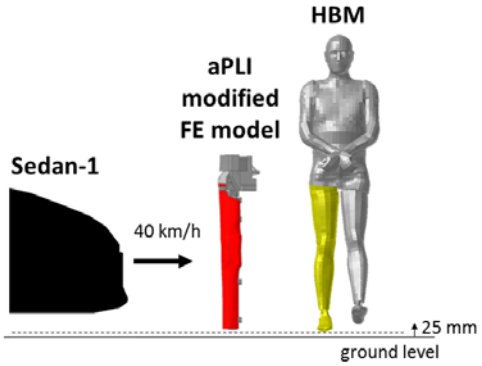

Fig. 2. CAE models and setting for 40 km/h lateral impact simulation against low-BLE car.

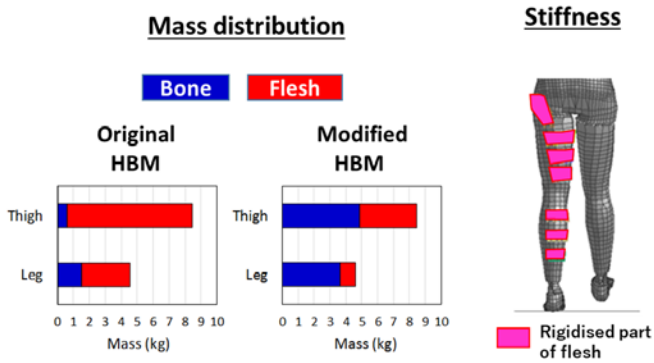

Fig. 3. Mass distribution and stiffness of bone and flesh for modified HBM.

Step 2: aPLI Modifications

2.1. Introduction of bumper system and determination of its specifications

Based on the hypothesis established and validated in Step 1, the simplest solution would have been to reduce the femur mass and the flesh stiffness of the aPLI. However, the aPLI is meant to be used in sub-system tests where the impactor is propelled into the front part of a car, and human-like light bone with soft flesh leads to large vibration during the launch, which compromises the impactor's repeatability and reproducibility.

Consequently, alternative aPLI modifications were investigated in detail to artificially mitigate the excess of energy stored in the upper part of the impactor.

The idea of the modification investigated was a bumper system (BS) attached to the base of the upper mass (Figure 4). This modification aimed at reducing the large femur BM, when the adduction angle surpassed a certain pre-defined angle. By introducing an angular gap between the bumper and the femur, the bumper activation timing can be controlled as it only works for hip adduction angles above the angular gap. Since there is a significant difference in maximum hip adduction angles between impacts with low-BLE (large angles) and high-BLE (small angles) cars, the BS would have a larger effect in impacts against low-BLE cars for which excessive peak injury measures are more evident, while having a less influence in high-BLE car impacts.

A BS FE model with tentative specifications was installed in the aPLI modified FE model (aPLI BS solid model (tentative specifications)) to qualitatively confirm its effectiveness by simulating an impact against the Sedan-1 model. The tentative BS specifications are shown in Appendix D. After the qualitative evaluation of the effectiveness of the BS, an aPLI modified FE model with a simplified BS represented by a joint element (aPLI BS joint model) was developed (Figure 5). The BS was modelled by the moment-angle characteristics of a cylindrical joint element specified at the hip joint. The angular gap and the bumper stiffness were represented by the onset angle of the moment and the slope of the subsequent moment-angle curve, respectively. Baseline joint characteristics (onset angle and slope) were determined from the BS FE model with the tentative specifications (Appendix D). The onset angle and the slope were tuned to have the desirable quantitative performance by conducting a numerical parametric study (range of parameters described in Table 1).

The target performance criterion was set at peak MCL elongation. As the knee is less stiff than the femur and the tibia, the energy storage and release of the femur and the resulting oscillation of tibia bending all influence the knee response in a later phase, resulting in a significantly larger peak value in low-BLE car impacts. A target range was determined for the mean ratio of peak MCL elongation between the aPLI BS joint model and the HBM across seven RCM impacts. The upper and lower limits of the mean ratio were set at 1.1 and 0.9, respectively. Since different combinations of the onset angle and the slope can produce the same MCL elongation, the combination with the largest slope was chosen among the combinations identified to meet the target, to reduce peak deflection of the BS upon a car impact and minimise the risk of buckling of the BS.

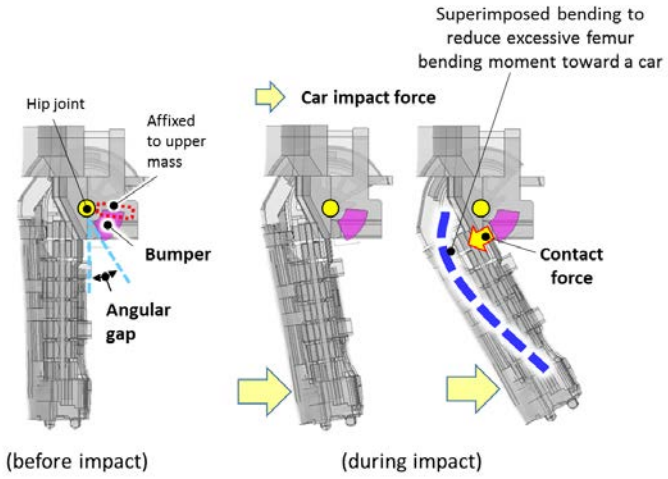

Fig. 4. Concept of bumper system (BS).

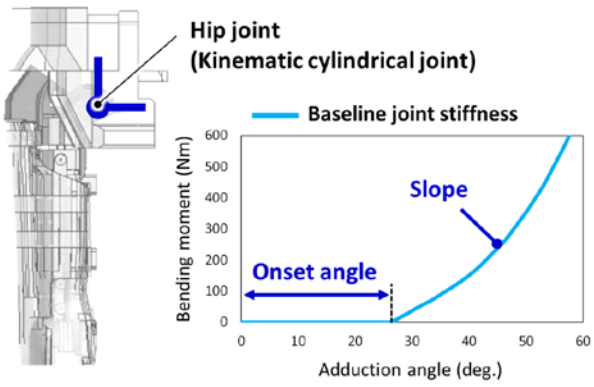

Fig. 5. Overview of aPLI BS joint model.

TABLE I
RANGE OF DESIGN PARAMETERS (ANGULAR GAP AND BUMPER STIFFNESS) OF APLI BS JOINT MODEL FOR PARAMETRIC STUDY

Angular gap (interval) (deg.)	Bumper stiffness ratio (interval) (bending moment scaling ratio against baseline joint stiffness)
0-25 (2.5)	0.5-2.0 (0.1)

2.2. Bumper system hardware design and fabrication

After finalising the BS specifications, a mechanical design of the BS was determined in such a way that the

addition of the BS would not yield any negative effect in actual car tests, including reduced repeatability, reproducibility and durability.

The design package of the BS was developed under the following conditions:

1. The moment-angle response represents the finalised BS specifications determined in Step 2.1
2. The BS is protected enough to avoid damage in a secondary impact (e.g. ground impact)
3. The most durable material is selected from available choices that meet other conditions
4. The BS allows stable compression of the bumper in car impacts with a safety margin

To conduct CAE analysis to determine the bumper shape and validate the finalised mechanical design in RCM impacts, numerical material parameters for a viscoelastic material model were determined for the selected bumper material to match the results of the dynamic compression tests. Ramp-and-hold tests were conducted at four loading rates (quasi-static, 0.01 strain/sec, 0.12 strain/sec and 9.59 strain/sec) by using test pieces (10 mm square, 4 mm thick) made of the selected material as illustrated in Figure 6. The dimensions of the bumper and the compression surface were tuned by a CAE analysis applying the material model for the bumper determined above. The final mechanical design of the BS was modelled and installed into the modified aPLI FE model (aPLI BS solid model (finalised specifications)), and its performance was evaluated by comparing injury measures against the HBM in the seven RCM impacts.

The mechanically designed and validated BS was fabricated and installed in the aPLI hardware unit (aPLI BS hardware unit). To experimentally validate its function, two types of inverse tests (Type 1 and 2) as shown in Figure 7 along with two car tests were conducted. First, in the inverse test Type 1, the aPLI hardware unit and the aPLI BS hardware unit were impacted at 40 km/h by a moving ram with a honeycomb just below the knee, as defined in the UN regulation for pedestrian safety [3-4]. In the inverse test Type 2, they were impacted at a location 120 mm above that of Type 1, to apply larger loads on the thigh. 3 tests were performed for each combination of the types of the test and the aPLI hardware unit. The two types of the inverse tests were also simulated using the aPLI modified FE model and the aPLI BS solid model (finalised specifications), and the time histories of the injury measures were compared with and without the BS for both the tests and the simulations to see if intended function of the aPLI BS solid model (finalised specifications) is represented by the fabricated aPLI BS hardware unit. In addition, the two types of inverse tests were simulated by using the HBM, to further validate the function of the BS. Second, 40 km/h aPLI impact tests using an aPLI hardware unit and an aPLI BS hardware unit were conducted against a low-BLE real sedan car at two different impact locations (two different lateral locations to the car where the BLE heights are 717 mm and 745 mm). The tests were performed in accordance with the UN global technical regulation for pedestrian safety [3], except for the impactor used (aPLI as opposed to FlexPLI) and impact height (25 mm above the ground level as opposed to 75 mm).

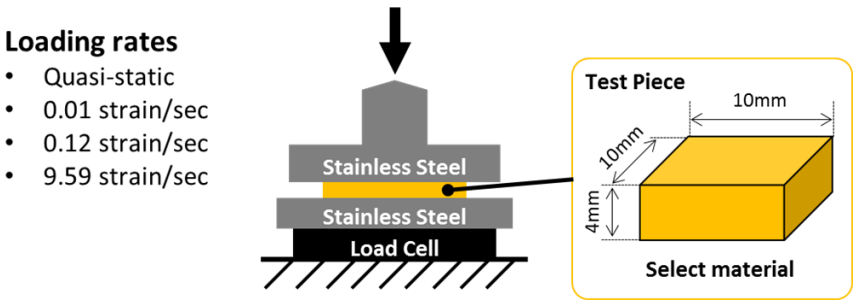

Fig. 6. Ramp-and-hold test conditions.

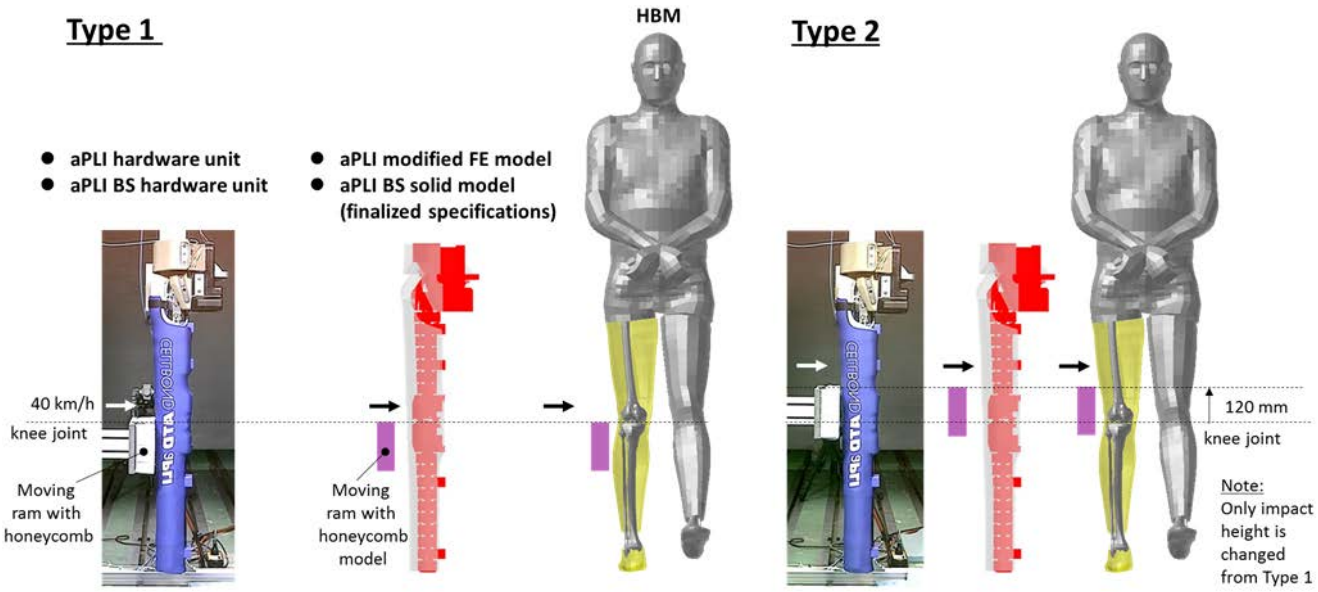

Fig. 7. aPLI inverse test (Type 1 and 2) and simulation setups.

III. RESULTS

Step 1: Analysis of Mechanism

Figure 8 shows the comparison of the injury measure time histories and kinematics from the HBM and the aPLI modified FE model in an impact with the Sedan-1 model. In comparison with the HBM, the aPLI modified FE model sustained a more pronounced femoral bending seen in a steeper onset and a larger bending moment at the upper part of the femur (Thigh-3 BM) at around 30 ms, followed by a large femur spring back that leads to a larger MCL elongation and a larger bending moment at the leg between 40 to 50 ms. Specifically, the secondary peak of Leg-1 BM in the rebound phase is larger than the initial peak that occurs during contact with the car, which clearly does not occur in the HBM. For this reason, focus will be given to Thigh-3 BM, MCL elongation and Leg-1 BM in the rest of the analysis.

The causation of the steeper onset and the larger magnitude of BM at the femur was assumed to be the heavier femur bone and the stiffer flesh of aPLI compared to those of a human (Appendix E). The heavier femur and the stiffer flesh of the aPLI tend to accumulate a larger bending energy in the femur compared to that of a human, and by releasing the energy in a spring back, excessive peak values in the rebound phase are reached. Specifically, the BLE of low-BLE cars do not contact the thigh of the aPLI. Due to the lack of constraint to the upper part of the thigh, the femur is free to bend, facilitating the presumed mechanism.

Figure 9 shows the results of the sensitivity study to investigate the influence of the difference of mass and stiffness of the bone and the flesh between the HBM and the aPLI modified FE model by artificially modifying mass distribution and flesh stiffness of the HBM. The modified HBM demonstrated a steeper onset and a larger magnitude of Thigh-3 BM compared to those of the original HBM, with similar trends to those of the aPLI modified FE model. Further, the modified HBM demonstrated a larger peak value of MCL elongation and a larger secondary peak value of Leg-1 BM compared to those of the original HBM, subsequently similar to those of the aPLI modified FE model.

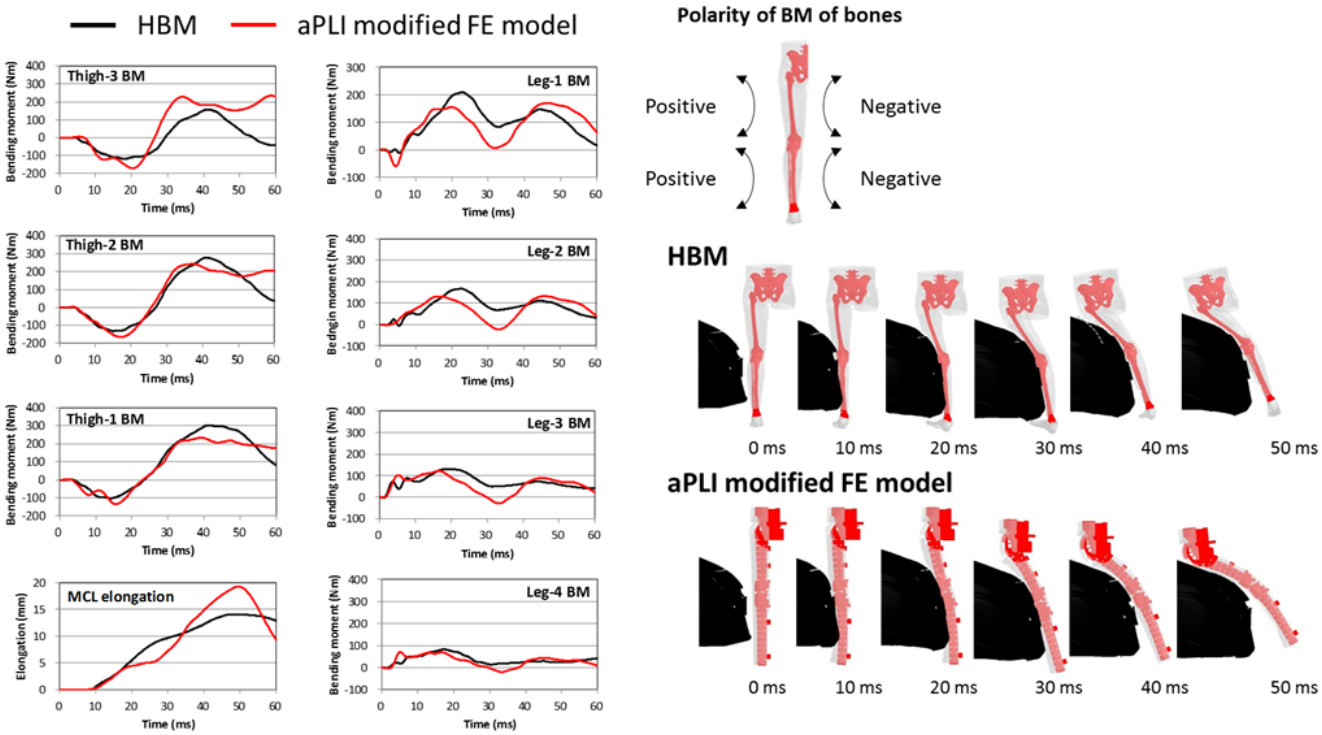

Fig. 8. Comparison of time history plots of Thigh BM (1-3), MCL elongation and Leg BM (1-4) and kinematics between HBM and aPLI modified FE model in impact with Sedan-1 model.

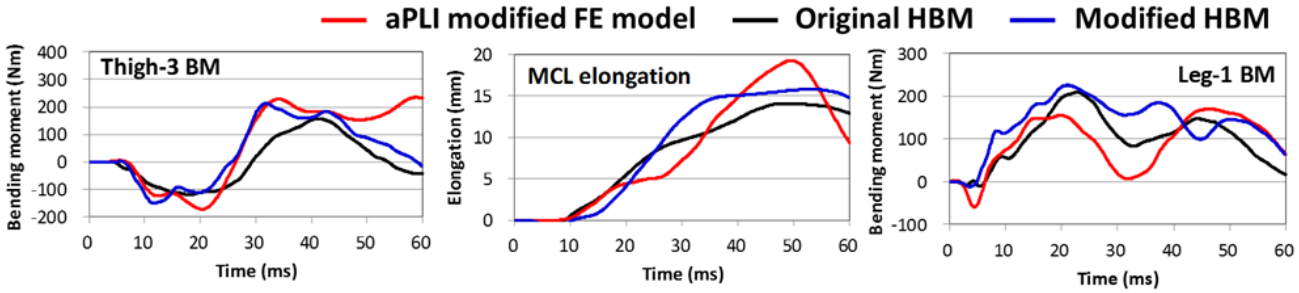

Fig. 9. Comparison of time history plots of Thigh-3 BM, MCL elongation and Leg-1 BM among aPLI modified FE model, original HBM and modified HBM in impact with Sedan-1 model.

Step 2: aPLI Modifications

2.1. Introduction of bumper system and determination of its specifications

The results of the qualitative sensitivity study to investigate the effectiveness of the BS with tentative specifications in an impact with the Sedan-1 RCM is shown in Figure 10. The aPLI BS solid model (tentative specifications) demonstrated a significant reduction of femur BM in the initial phase at around 30 ms, followed by a reduction of the peak MCL elongation and the peak leg BM between 40 to 50 ms.

Figure 11 shows the performance of the aPLI BS joint model (finalised specifications; onset angle = 2.5 degrees and slope = 1.8 times that of the baseline shown in Figure 5) from impact simulations with the seven RCMs. The mean ratio of the peak MCL elongation from the aPLI BS joint model (finalised specifications) to that from the HBM in seven RCM impacts was 1.01, which meets the target range (0.9 to 1.1). In addition, the finalised specifications also improved the correlation of thigh BM and leg BM between the aPLI BS joint model (finalised specifications) and the HBM, with the regression lines getting closer to equality.

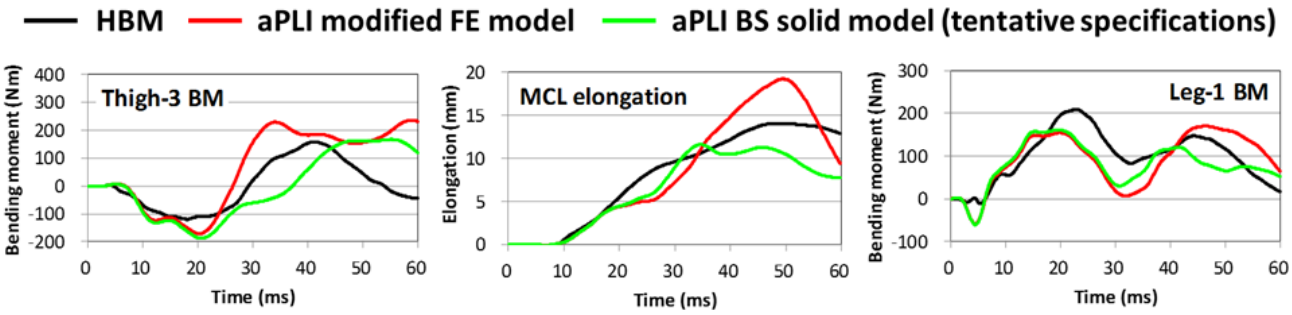

Fig. 10. Comparison of time history plots of Thigh-3 BM, MCL elongation and Leg-1 BM among HBM, aPLI modified FE model and aPLI BS solid model (tentative specifications) in impact with Sedan-1 RCM.

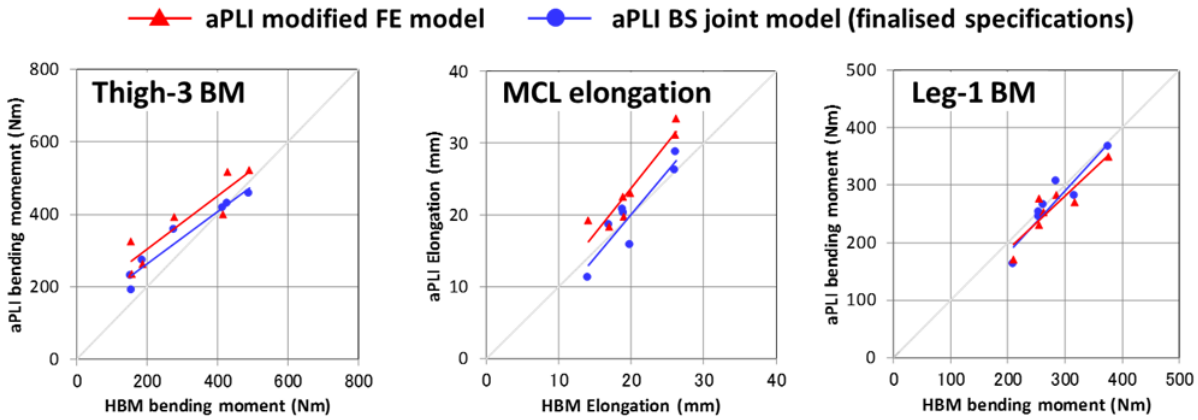

Fig. 11. Correlation of peak values of Thigh-3 BM, MCL elongation and Leg-1 BM between HBM and two aPLI models (aPLI modified FE model and aPLI BS joint model (finalized specifications)) in seven RCM impacts.

2.2. Bumper system hardware design and fabrication

Figure 12 shows the schematic image of the initial mechanical design idea and its working mechanism of the BS. The BS is completely installed inside of the UM to avoid the risk of damage to the bumper in a secondary impact (e.g. ground impact). The bumper is compressed by the compression surface of the femur top mounting bracket in hip adduction, the reaction force being transmitted to the femur via the femur top mounting bracket in the form of moment about the hip joint in the negative direction (see Figure 8 for polarity).

With regard to the bumper material, urethane 75 Shore A was selected because of its high tensile strength and durability relative to other rubber materials [14]. In fact, it demonstrated a highly durable performance in our material testing where a rectangular solid test piece of the same material was subjected to one hundred quasi-static and subsequently fifty dynamic compression tests (Appendix F). Figure 13 compares the stress-strain and stress-time plots obtained from the ramp-and-hold tests of the material chosen for the bumper (urethane 75 Shore A) with those from numerical simulations. The material parameters tabulated in table 2 are optimised values to match the test results. Aluminium was chosen for the material of the femur top mounting bracket and the bumper mount to minimise their weight while ensuring durability in car tests.

A number of design iterations were run between computational performance evaluation and mechanical design modifications to come up with a finalised design of the BS. The final design reached is shown in Figure 14. The dimensions of the bumper and the compression surface were determined to avoid buckling, slipping and edge contact up to 27 degrees of the hip adduction angle. This angle is 1.2 times larger than the maximum hip adduction angle occurring in seven RCM impacts for a safety margin (Appendix G).

Figure 15 shows the results of the impact simulations with the seven RCMs for the HBM and the two different aPLI models (aPLI BS joint model (finalised specifications) and aPLI BS solid model (finalised specifications)). The deviations of the peak MCL elongation between the two models ranged 0.1 - 3.2 % (average 1.1 %).

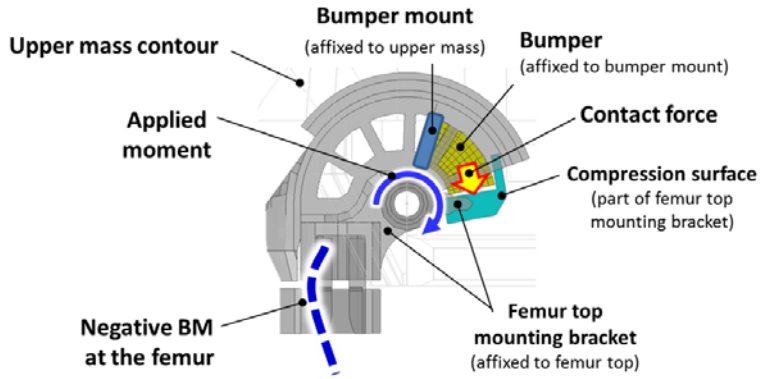

Fig. 12. Schematic image of initial mechanical design idea of BS and its working mechanism.

TABLE II
MATERIAL PARAMETERS FOR BUMPER MODEL

Material type (-)	Bulk modulus (MPa)	Short-time shear modulus (MPa)	Long-time shear modulus (MPa)	Decay constant (s^{-1})
Linear viscoelastic for sold element (Type 5)	40	7	2.7	1

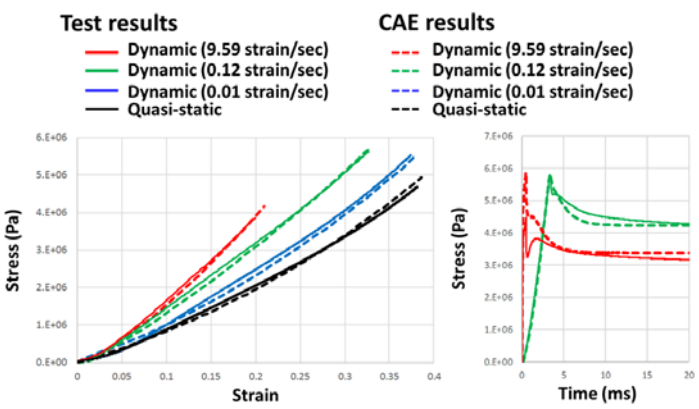

Fig. 13. Comparison of stress-strain and stress-time plots in quasi-static and dynamic ramp-and-hold compression between experiment and simulation.

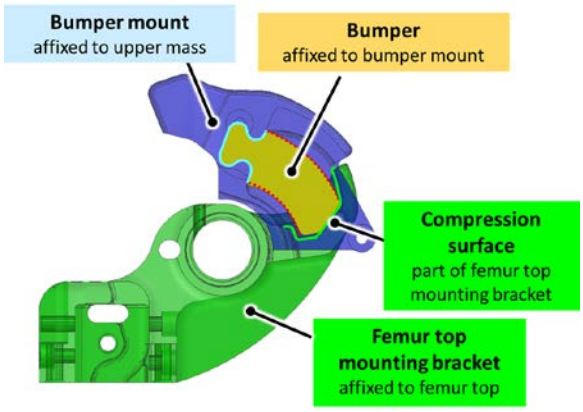

Fig. 14. Final mechanical design of BS.

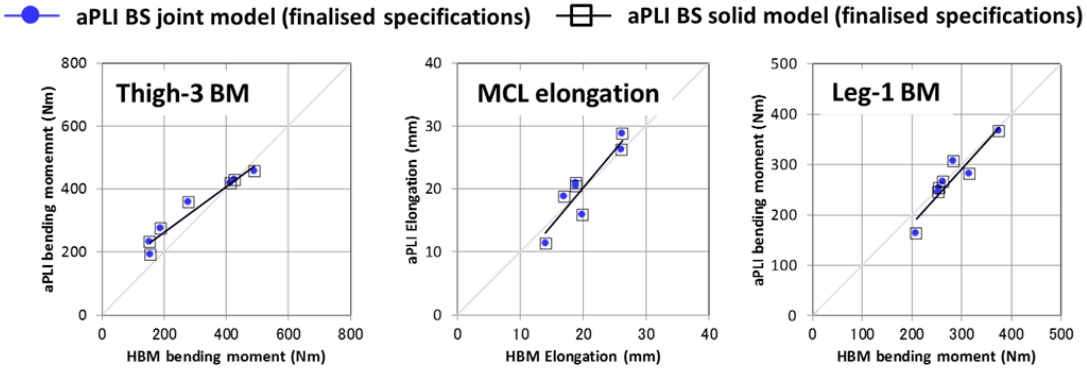

Fig. 15. Comparison of peak values of Thigh-3 BM, MCL elongation and Leg-1 BM between HBM and two aPLI models (aPLI BS joint model (finalised specifications) and aPLI BS solid model (finalised specifications)) in seven RCM impacts.

The BS with the final design was fabricated (Figure 16) and installed in an aPLI BS hardware unit. Figure 17 compares time histories of Thigh-3 BM, MCL elongation and Leg-1 BM among the aPLI modified FE model, aPLI BS solid model (finalised specifications) and HBM obtained from inverse test (Type 1 and 2) simulations. Figure

18 compares the same among the aPLI hardware unit, aPLI BS hardware unit and HBM obtained from inverse tests (Type 1 and 2). In both the simulations and the tests, the BS reduces femur BM around 20 to 30 ms, resulting in lower values of MCL elongation and leg BM in the later phase. Those figures also demonstrate that the time history plots from the aPLI with the BS better represent those from the HBM in both the FE model and the hardware unit, specifically for Thigh-3 BM (Type 1 and 2) and Leg-1 BM (Type 1) where significant difference in the time history plots can be seen with and without the BS.

Figure 19 shows the time histories of Thigh-3 BM, MCL elongation and Leg-1 BM for the aPLI hardware unit and the aPLI BS hardware unit in car tests. The aPLI BS hardware unit clearly demonstrated a lower MCL elongation and leg bending moment in the rebound phase than those of the aPLI hardware unit due to the effect of the BS that reduced femur bending moment.

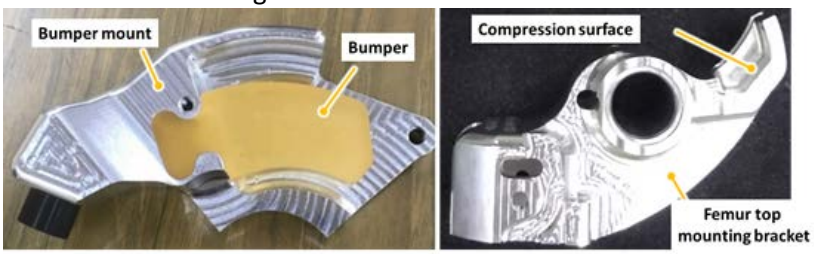

Fig. 16. Fabrication of mechanically designed BS (unfinished surface for prototype).

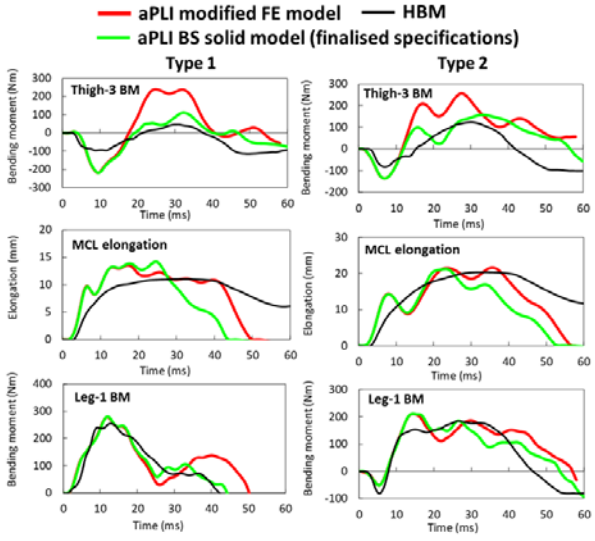

Fig. 17. Comparison of time histories of injury measures among aPLI modified FE model, aPLI BS solid model (finalised specifications) and HBM in inverse (Type 1 and 2) test simulations.

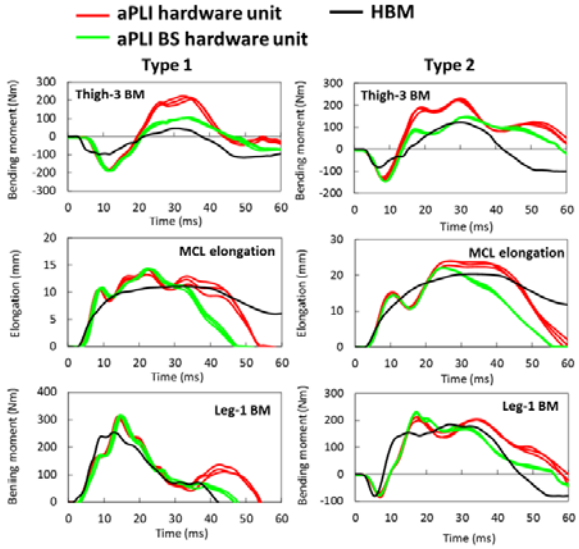

Fig. 18. Comparison of time histories of injury measures among aPLI hardware unit, aPLI BS hardware unit and HBM in inverse (Type 1 and 2) tests (n=3) and simulations.

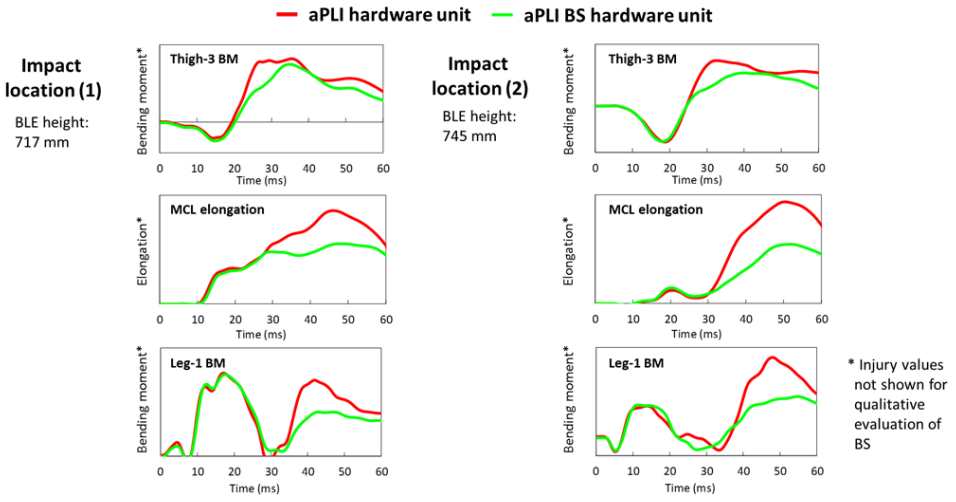

Fig. 19. Comparison of time histories of Thigh-3 BM, MCL elongation and Leg-1 BM between aPLI hardware unit and aPLI BS hardware unit in real car tests.

IV. DISCUSSION

The biofidelity of the aPLI in the rebound phase was improved using a 2-step approach. In the first step, the mechanism of the excessive peak values of the injury measures was investigated for the aPLI in the rebound phase in an impact against a low-BLE car. As a result, it was clarified that the heavier femur and the stiffer flesh of the aPLI compared to those of a human are responsible for the steeper onset and the larger magnitude of the bending moment at the femur compared to those of the HBM, via the accumulation of a larger bending energy at the femur during the impact, and the release of the energy when the femur springs back. This spring back ultimately induces an excessive peak injury value in the rebound, in particular, for the MCL. The combination of a heavier femur and the stiffer flesh of the aPLI, compared to those of humans, is a required trade-off solution between biofidelity and repeatability of tests. A purely human-like combination of lighter bone and softer flesh could potentially enhance the biofidelity of the impactor. However, such a modification would, in practice, induce large vibrations during the high-acceleration launches of the impactor, which would in turn sacrifice repeatability of the test results using the impactor. This situation would also apply to other impactors and/or anthropomorphic test devices (ATDs) if compliant bony structures were introduced. The results of the current study provide insight into the difference in the impact response of ATDs and human bodies, whose mass distributions between bones and surrounding soft tissues are significantly different.

After the clarification of the mechanism of the generation of excessive peak values, an additional measure to reduce the excessive peak values in the rebound phase was investigated. The concept of the measure is to externally apply force on the femur in the direction to cancel the BM generated by the impact kinematics.

The initial idea was to add a rotational mass damper, consisting of a mass and a rotational spring attached to the upper part of the femur. Although this modification succeeded in reducing the energy accumulated by the femur, the spring back of the rotational mass damper negatively influenced femur BM in a later phase. After the consideration, the BS was found to realise the desired functions because it works to cancel part of the large femur energy only in the early phase of the car impact, with no influence in the late phase at all after the bumper loses contact with the compression surface. The hardest challenge in this development was that the additional component needed to have a limited effect in most load cases, except for impacts against some specific low-BLE cars, while influencing only a specific time domain of the femur bending response even in such specific load cases. The first key point was that the BS makes the best use of the difference in the hip adduction angle response between low- and high-BLE cars. The system applies a magnitude of force enough to influence the original bending response due to impact kinematics only when the hip adduction angle reaches a certain amount. As this can be realised only in impacts against specific low-profile cars where the femur of the aPLI largely rotates toward the bonnet of the cars due to the low BLE, it does not have any significant influence on other load cases, avoiding deterioration of improved biofidelity achieved by the aPLI. In addition, the tuning of the angular gap between the bumper and the femur was another key that allowed adjustment of the onset timing of the additional load provided by the BS. These two key points were inevitable for addressing the issue of the response in the rebound phase predominant in limited and specific load cases and a time domain. It should also be noted that due to the external loading exerted on the femur, for some limited load cases, the mechanism achieving a similar peak MCL elongation differs from that in the case of the HBM. Thus, the biofidelity of the aPLI with the BS is limited, for the limited load cases addressed by the additional system, to the correlation of peak values of the injury measures, with slightly different waveforms of the injury measure time histories (Appendix H).

The BS was mechanically designed for implementation in the aPLI hardware unit. First, desirable specifications of the BS were determined by lumping the bumper characteristics into the hip joint (aPLI BS joint model) and performing a parametric study by setting the onset angle and the slope as design parameters. The determined bumper characteristics identified were then transformed into an FE model of the bumper and associated brackets. The reduction in femur BM and MCL elongation seen in the inverse tests conducted using the aPLI modified FE model and the aPLI BS solid model (finalised specifications) were accurately reproduced in subsequent inverse tests and low-BLE car tests. This match was obtained without any iteration, suggesting that the modelling technique, including the material characterisation of the urethane comprising the bumper, has now become a powerful tool to design ATDs and accurately predict their performance. The aPLI has been a pioneering example of intensively utilising FE models and computer simulations in its design and performance validation, which is one of the unique features of its development.

In this study, only seven RCMs were used to confirm the validity of the BS solution proposed and the robustness of the results require further verification. It should also be noted that the inverse test setups used in this study as part of the functional evaluation do not provide ideal load cases as the legform is loaded only at one single location and thus the internal load transmission would be significantly different from that in car impacts. Further evaluation of the validity of the BS performance with other cars in international round-robin tests will shed light on the applicability of the BS solution. The aPLI BS solid model (finalised specifications) and the aPLI BS hardware unit show slight differences when compared directly in the inverse test conditions (Type 1 and 2) (Appendix I), which might require future fine tuning of the BS response. No FE simulations were conducted to reproduce the car tests performed to evaluate the function provided by the BS. In the course of the future international round-robin tests, some of the car impacts need to be computationally simulated using the HBM and the aPLI model to further validate the BS developed in the current study.

V. CONCLUSIONS

The heavier bone and the stiffer flesh of the aPLI compared to those of humans are the main cause of the mechanism that produces excessive peak values of MCL elongation and leg bending moment of the aPLI in the rebound phase predominant in impacts with cars with a low-bonnet leading edge. A bumper system that works in hip joint adduction installed inside the upper mass at the hip joint addresses this issue, without sacrificing any of aPLI's biofidelity at early impact stages or with higher bonnet leading edge cars.

VI. REFERENCES

[1] Mizuno Y. Summary of IHRA pedestrian safety WG activities (2005) Proposed test methods to evaluate pedestrian protection afforded by passenger cars. *Proceedings of 19th ESV Conference*, 2005, Paper Number 05-0138.
[2] ITARDA. "Statistics of traffic accident data in Japan, in Japanese, 2017" Internet: https://www.itarda.or.jp/materials/traffic/free, Cited 2020 June.
[3] United Nations. "Global Technical Regulation (GTR) No.9 (Pedestrian safety) Amendment 2" Internet: http://www.unece.org/trans/main/wp29/wp29wgs/wp29gen/wp29glob_registry.html, Cited 2020 June.
[4] United Nations. "Regulation (R) No. 127 - Rev.2 – Pedestrian safety" Internet: http://www.unece.org/trans/main/wp29/wp29regs121-140.html, Cited 2020 June.
[5] Isshiki, T, Konosu A, Takahashi Y. Influence of the upper body of pedestrians on lower limb injuries and effectiveness of the upper body compensation method of the FlexPLI. *Proceedings of SAE World Congress*, 2015, Paper Number 2015-01-1470.
[6] OICA. "GRSP-57-12: Pedestrian safety bumper test area" Internet: https://www.unece.org/trans/main/wp29/wp29wgs/wp29grsp/grspinf57.html, Cited 2020 June.
[7] Perez R D, Forman J L, Jeon H, Crandall J R. External biofidelity of Flex - PLI compared to the THUMS pedestrian model. *Proceedings of IRCOBI Conference*, 2016, IRC-16-67.
[8] OICA. "GTR9-5-08: Proposal for procedure to process FlexPLI measurements in rebound phase" Internet: https://wiki.unece.org/display/trans/GTR9-2+5th+session, Cited 2020 June.
[9] Isshiki T, Antona-Makoshi J, Konosu A, Takahashi Y. Optimal specifications for the advanced pedestrian legform impactor. *Stapp Car Crash Journal*, 2017, Vol. 61, pp. 373-395.
[10] Isshiki T, Konosu A, Antona-Makoshi J, Takahashi Y. Consolidated technical specifications for the advanced Pedestrian Legform Impactor (aPLI). *Proceedings of IRCOBI Conference*, 2018, IRC-18-42.
[11] Takahashi Y, Kikuchi Y, Mori F, Konosu A. Advanced FE lower limb model for pedestrians. *Proceedings of 18th ESV Conference*, 2003, Paper Number 218.
[12] Kikuchi Y, Takahashi Y, Mori F. Development of a finite element model for a pedestrian pelvis and lower limb. *SAE Technical Paper*, 2006-01-0683.
[13] Takahashi Y, Suzuki S, Ikeda M, Gunji Y. Investigation on pedestrian pelvis loading mechanisms using finite element simulations. *Proceedings of IRCOBI Conference*, 2010.
[14] Editorial board of dictionary of polymer technology. Dictionary of polymer technology. *Taiseisha*, 2011.

APPENDIX A: APLI MODIFIED FE MODEL

The aPLI modified FE model was developed by referring to design details of an aPLI hardware unit. The aPLI modified FE model was validated by comparing its response to experimental data, including quasi-static 3-point bending certification tests of the thigh, knee and leg, and dynamic full-assembly certification tests (inverse tests (Type 1 and 2)).

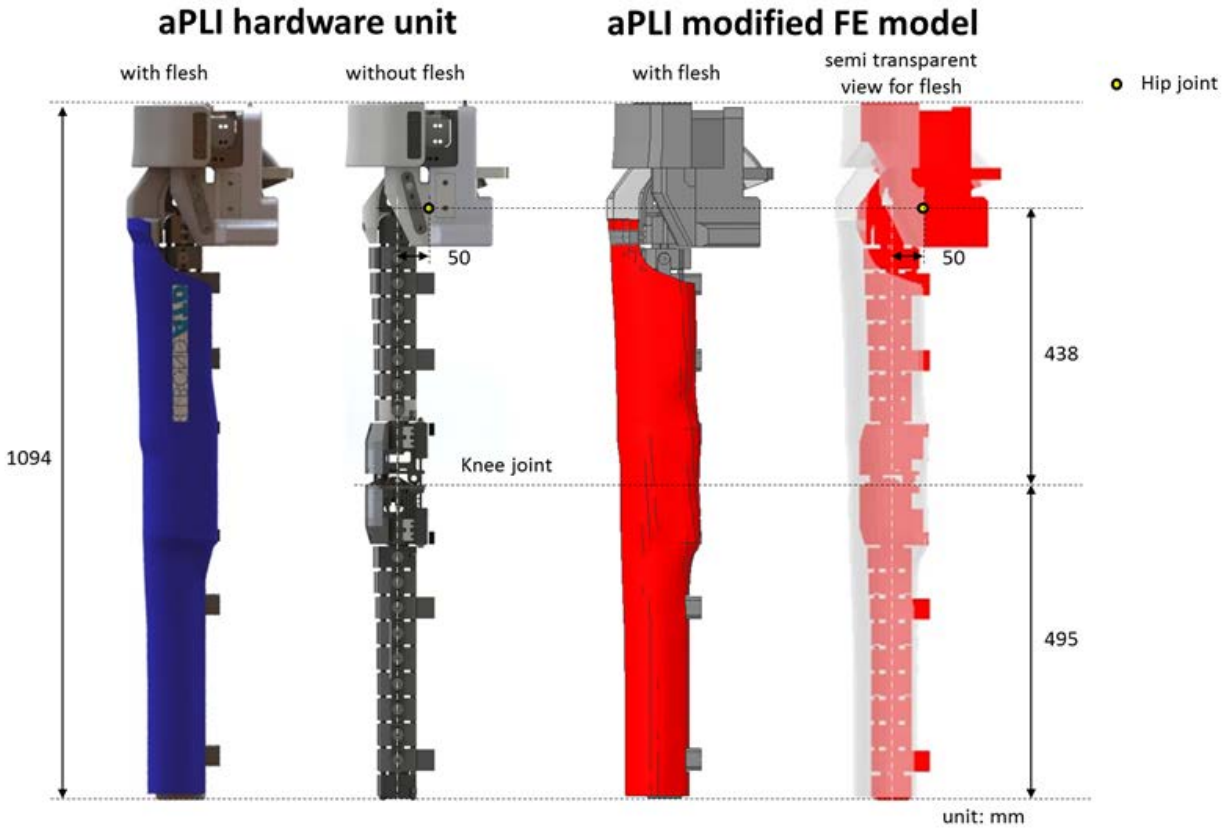

Fig. A1. Outer view of aPLI hardware unit and aPLI modified FE model.

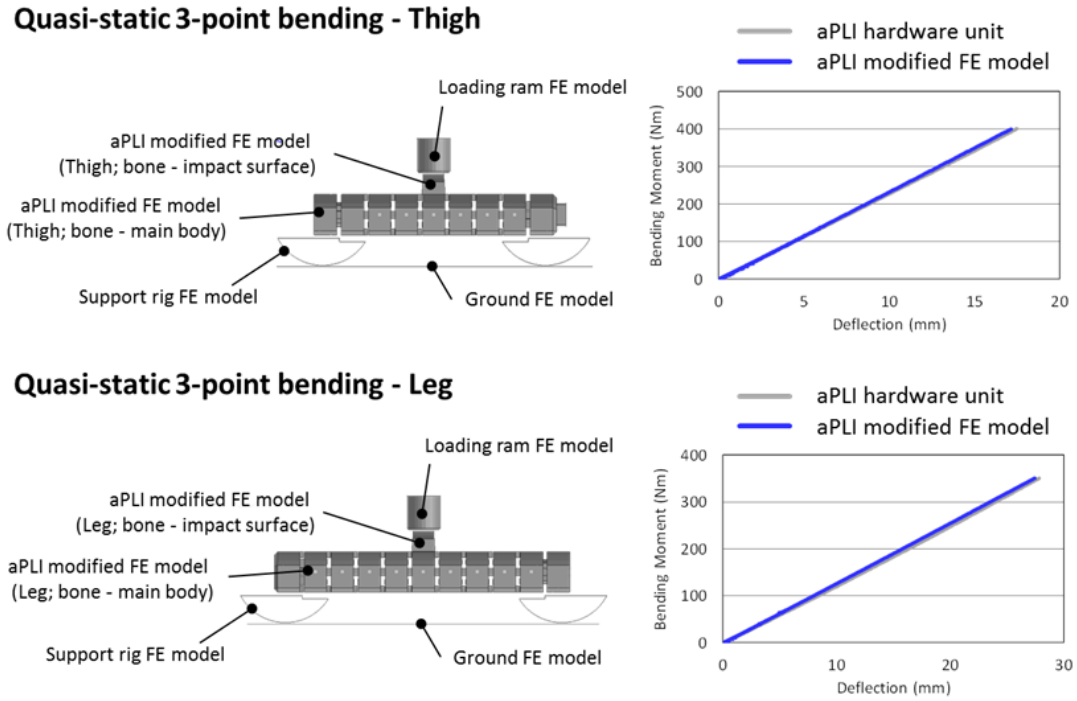

Fig. A2. Comparison of bending moment-deflection plots in Thigh and Leg quasi-static 3-point bending between aPLI hardware unit and aPLI modified FE model.

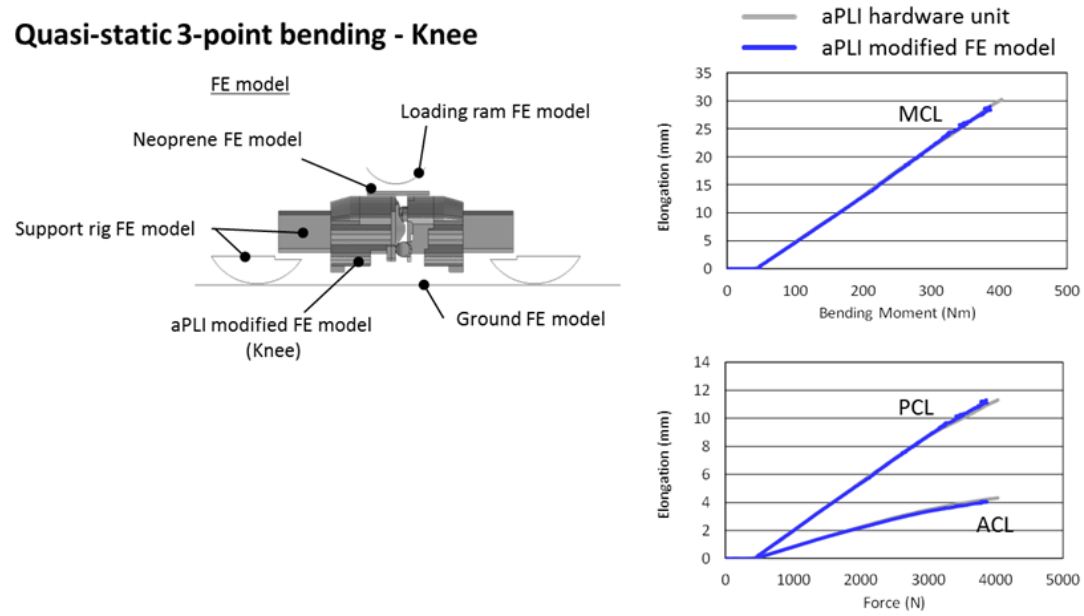

Fig. A3. Comparison of MCL elongation-bending moment and ACL/PCL elongation-force plots in knee quasi-static 3-point bending, between aPLI hardware unit and aPLI modified FE model.

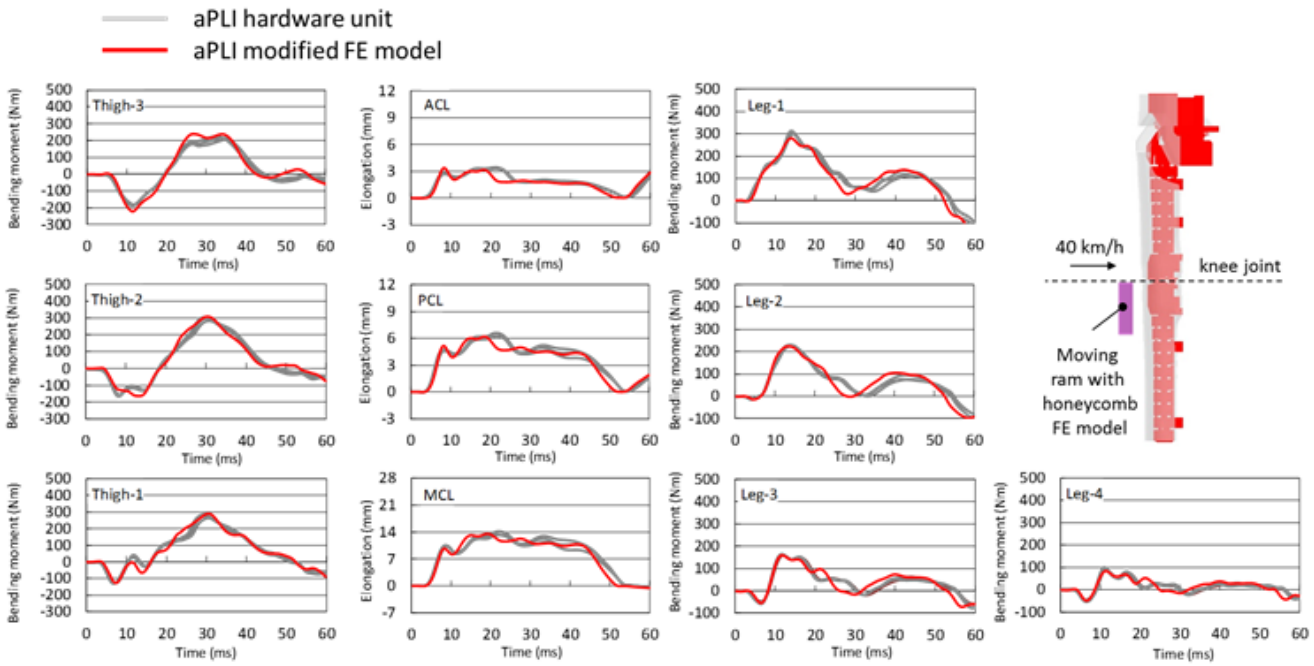

Fig. A4. Comparison of time histories of Thigh BM, ACL/PCL/MCL elongation and Leg BM between aPLI hardware unit (n=3) and aPLI modified FE model in inverse test and simulation (Type 1).

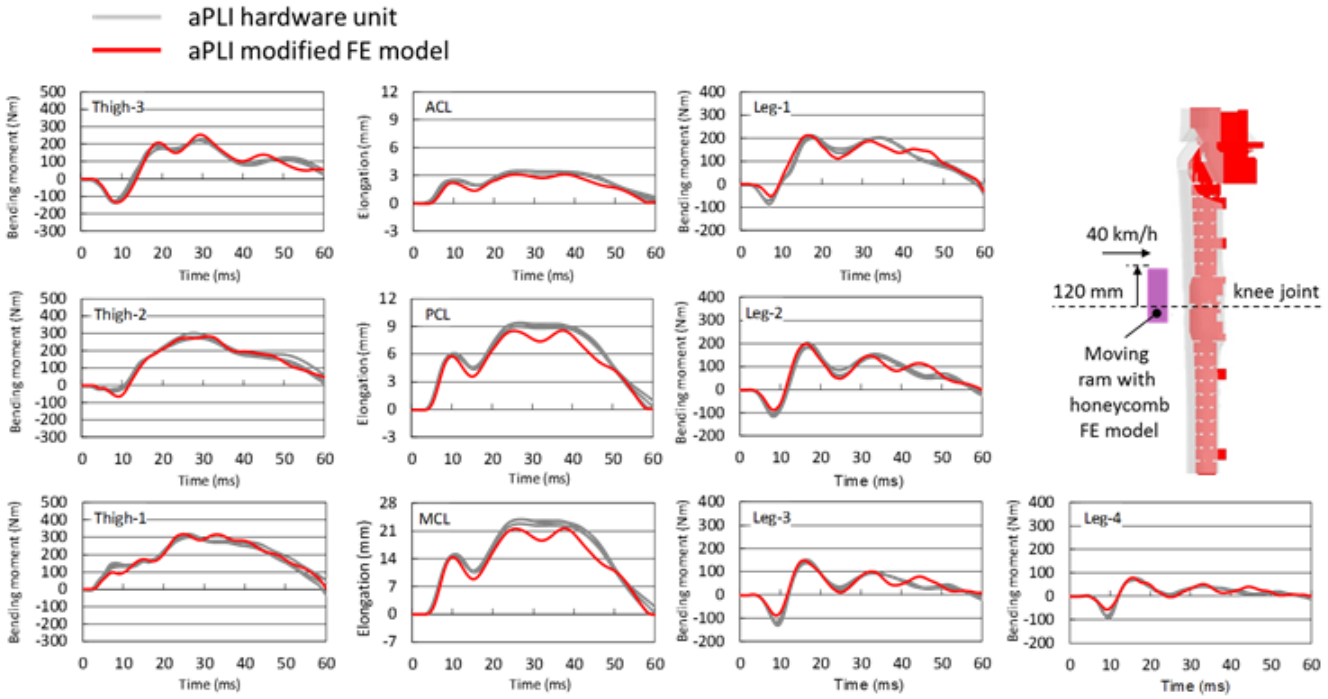

Fig. A5. Comparison of time histories of Thigh BM, ACL/PCL/MCL elongation and Leg BM between aPLI hardware unit (n=3) and aPLI modified FE model in inverse test and simulation (Type 2).

APPENDIX B: INFLUENCE OF CONTACT SETTING BETWEEN LOWER LIMBS OF HBM

Influence of the contact setting between the bilateral lower limbs of the HBM on peak values of injury measures is shown below. The contact setting between the lower limbs was not considered in this study because its influence on the peak value of injury measures was found to be small, and it is impossible to mimic the contact using the aPLI with a single lower limb.

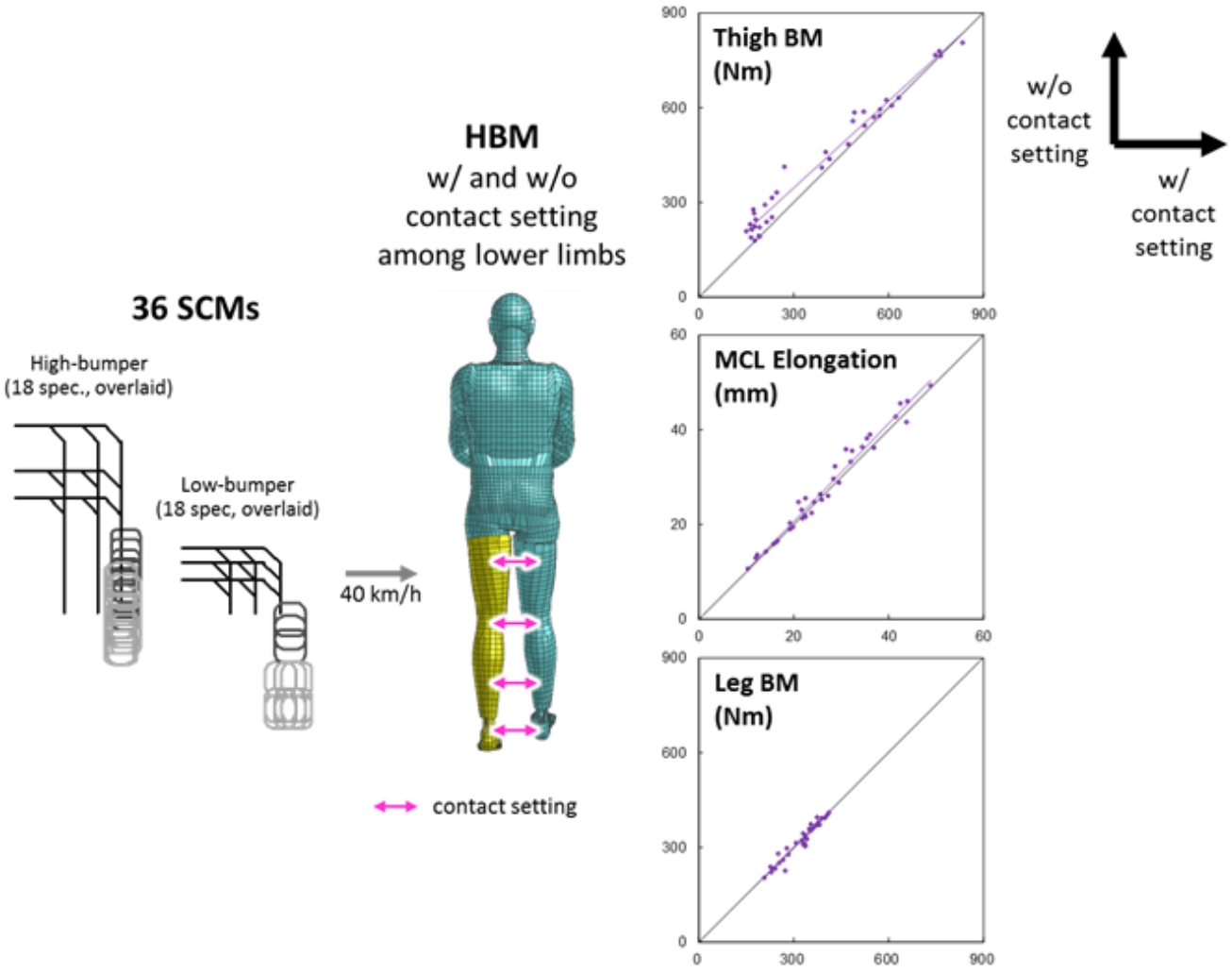

Fig. B1. Correlation of peak values of Thigh BM, MCL elongation and Leg BM with and without contact setting in 36 SCM [10] impact simulations.

APPENDIX C: MEASUREMENT LOCATIONS

Measurement locations of bending moment of bones and MCL elongation for the HBM and the aPLI modified FE model are described below.

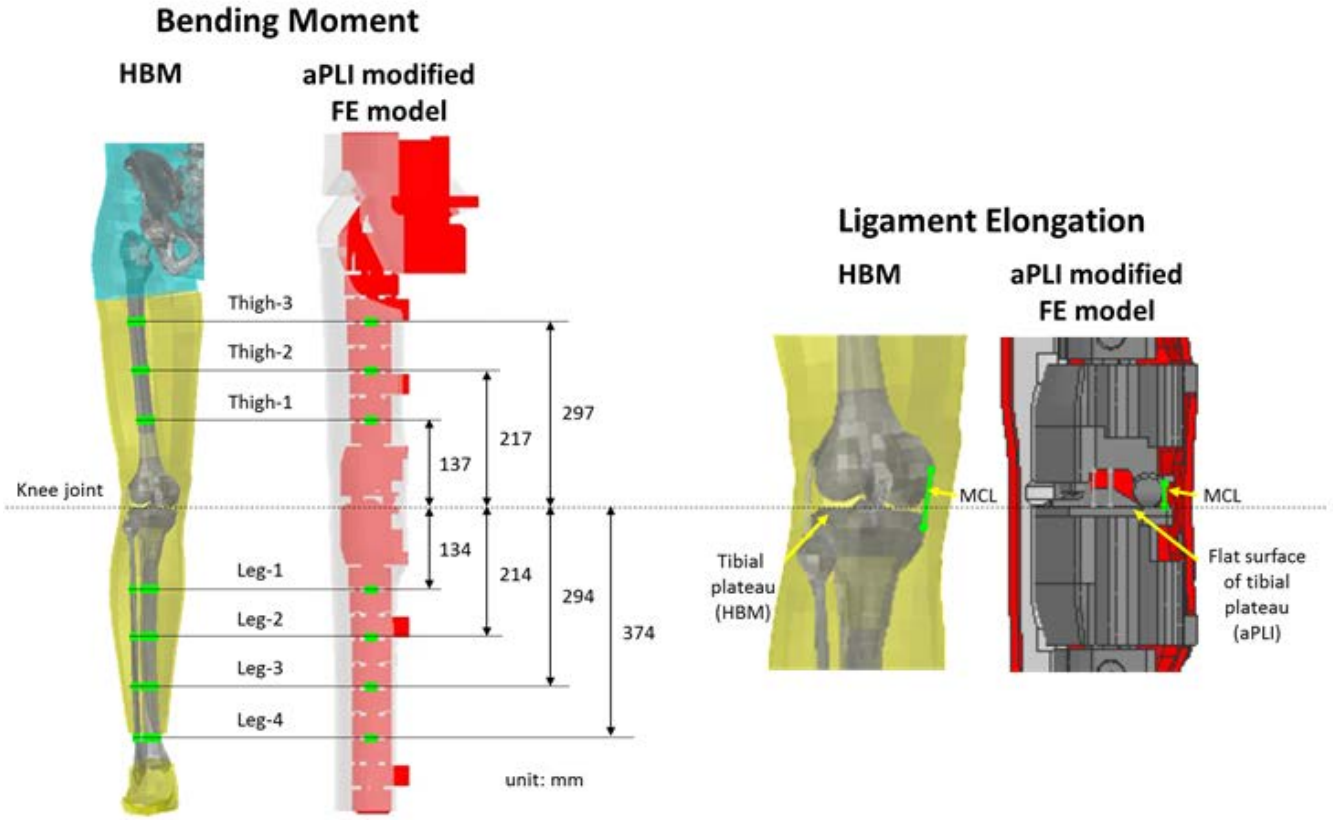

Fig. C1. Injury measurement locations for HBM and aPLI modified FE model.

APPENDIX D: BS FE MODEL WITH TENTATIVE SPECIFICATIONS

Tentative specifications of the BS FE model were determined from an FE model of an existing rubber material to evaluate the effectiveness of BS qualitatively.

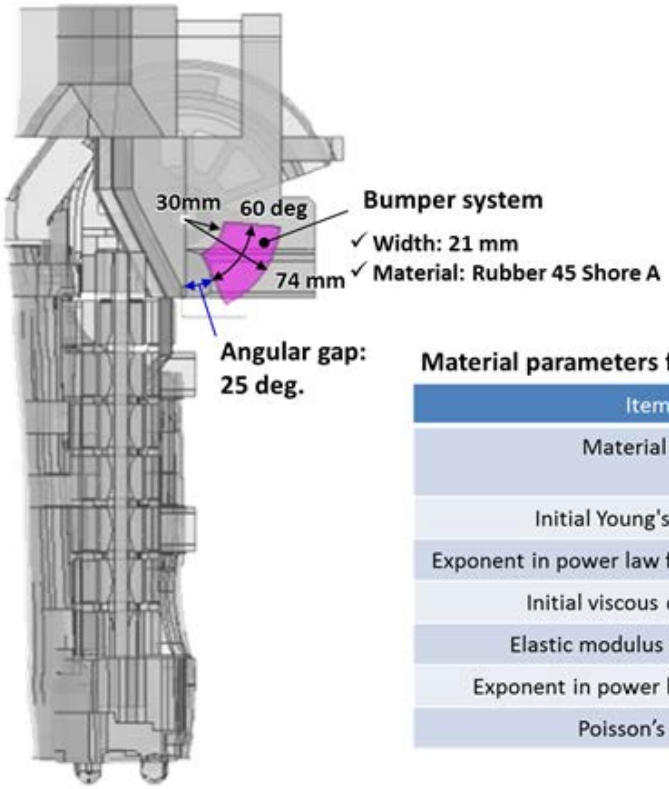

Material parameters for Rubber 45 Shore A FE model

Item	unit	Contents
Material card	-	Non-linear viscoelastic for solid element (Type 22)
Initial Young's modulus	(MPa)	2.0
Exponent in power law for Young's modulus	(-)	0.0
Initial viscous coefficient	(MPa·s)	35.0
Elastic modulus for viscosity	(MPa)	3.0
Exponent in power law for viscosity	(-)	0.75
Poisson's ratio	(-)	0.4

Fig. D1. Tentative specifications for BS.

APPENDIX E: COMPARISON BETWEEN HUMAN AND APLI

The mass and the stiffness of the entire lower limb of the aPLI modified FE model are similar to those of the HBM, resulting in similar natural frequency as shown in Figure E1. However, the mass and the stiffness distributions of the aPLI modified FE model between the bone and the flesh are different from those of the HBM as shown in Figure E2. Because the aPLI is designed to be used in subsystem tests where the impactor is propelled into the front part of a car, light bone and a soft flesh as in a human would lead to large vibrations during the launch, causing low repeatability and reproducibility. On the other hand, the natural frequency of the entire lower limb needs to be similar to that of a human to allow injury assessment using injury measure time histories. For these reasons, heavier bone and stiffer flesh need to be chosen for the aPLI.

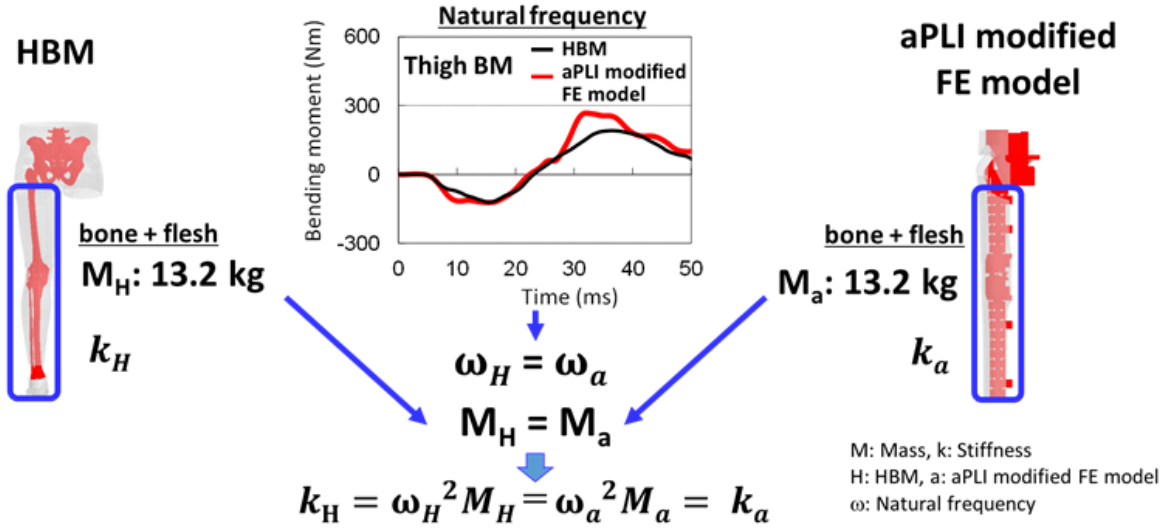

Fig. E1. Comparison of natural frequency, mass and stiffness of entire lower limb between human and aPLI.

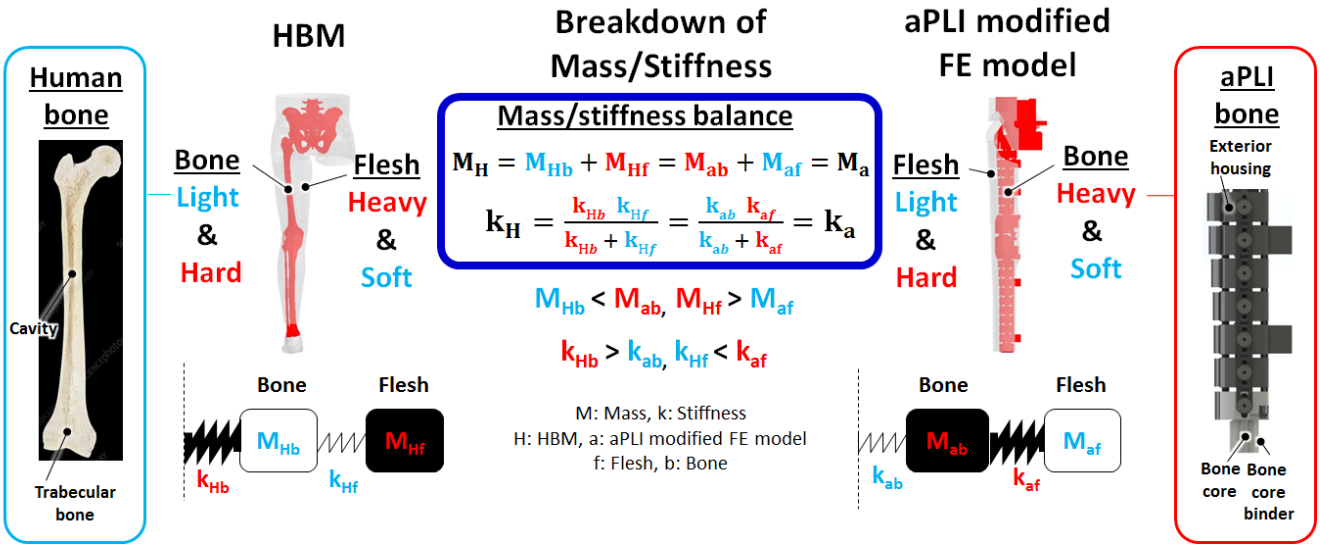

Fig. E2. Comparison of mass and stiffness of bone/flesh between human lower limb and aPLI.

APPENDIX F: DURABILITY OF URETHANE 75 SHORE A

Durability tests of urethane 75 Shore A were conducted as shown in Figure F1. First, its initial stress-strain curve was obtained in a quasi-static compression test at 0.1 strain/sec up to 0.4 strain. Second, 100 sequential quasi-static compression tests were conducted at 0.1 strain/sec up to 0.4 strain. Third, 50 sequential dynamic drop tests (weight: 5.12 kg , diameter of impact surface: 75 mm, drop height: 300 mm, maximum strain: around 0.4) were performed. After all those tests, the final quasi-static compression test was run again to compare the stress-strain curve against the initial test, confirming high durability of the material chosen.

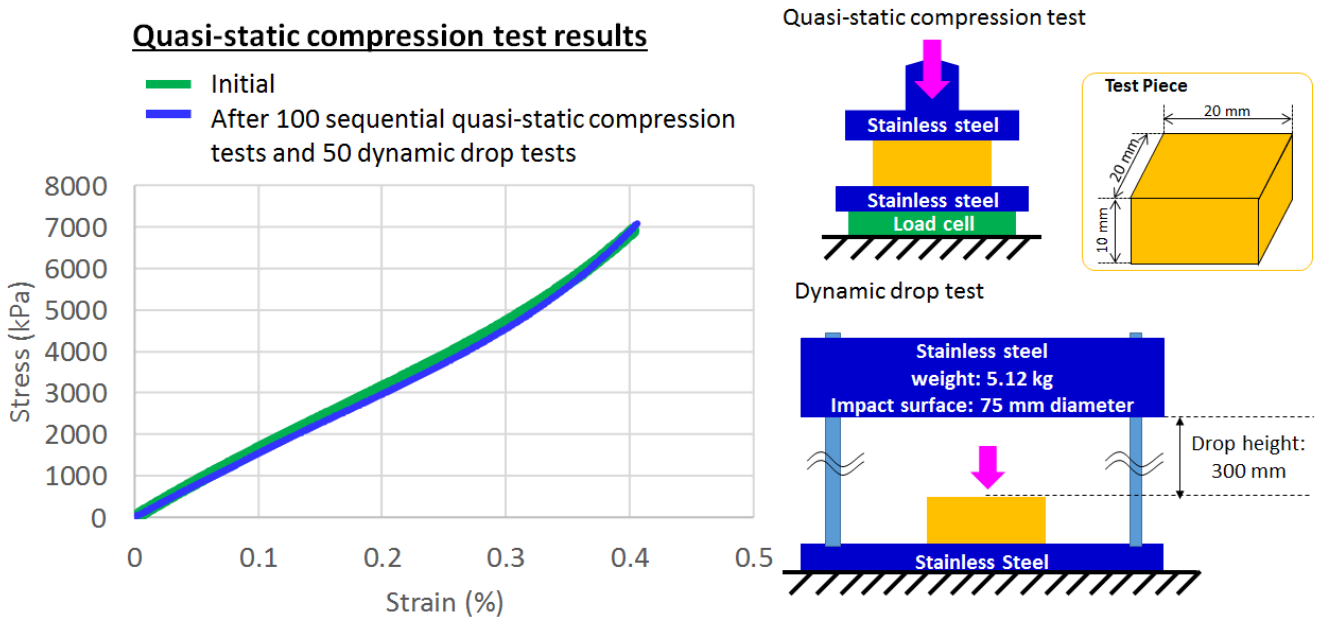

Fig. F1. Comparison of stress-strain curve in quasi-static compression test of urethane 75 shore A material between initial and final tests.

APPENDIX G: TIPS FOR OPTIMIZATION OF SHAPES

The shape of the bumper and compression surface were determined to avoid buckling, slipping and edge contact during car tests. In addition, by introducing a key slot design at the bumper mount, easy installation of the bumper was achieved.

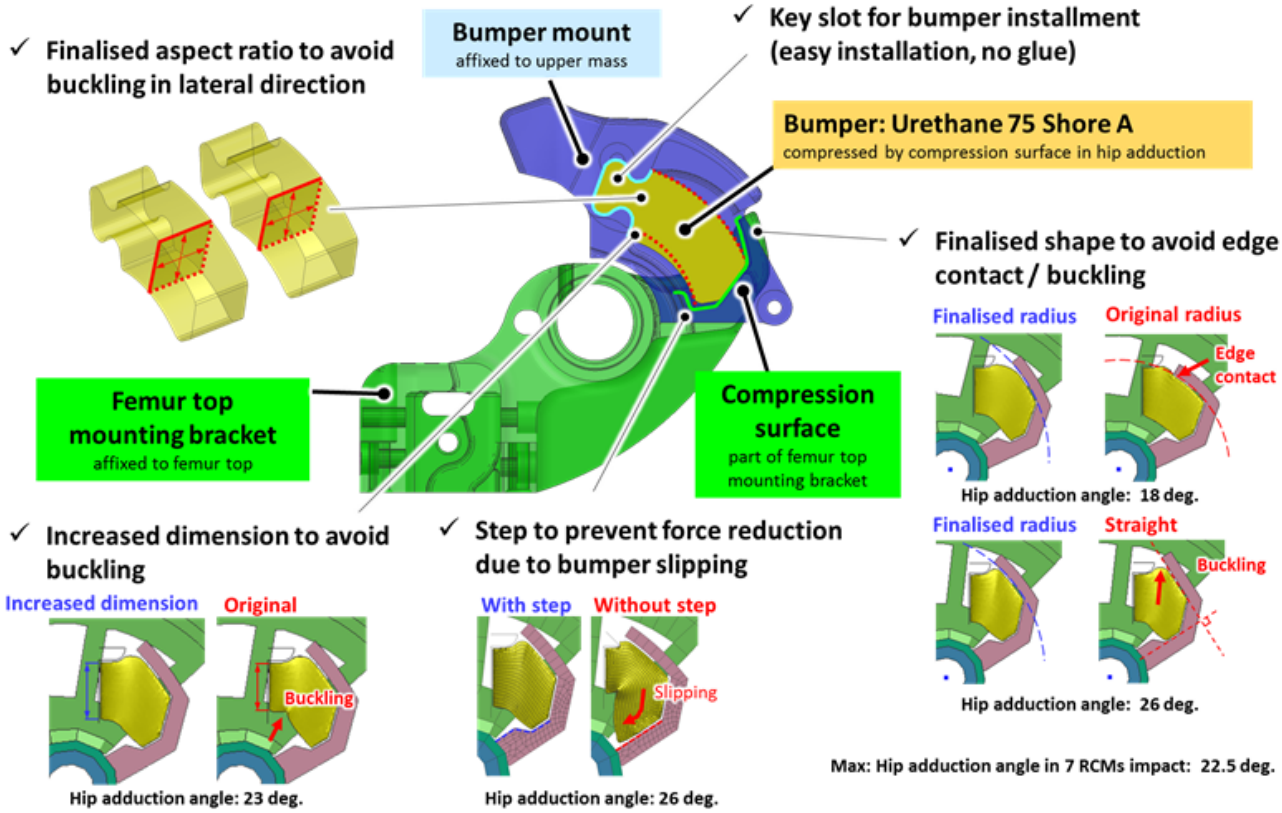

Fig. G1. Tips for optimization of shape of bumper and compression surface.

APPENDIX H: TIME HISTORY PLOTS OF HBM, APLI MODIFIED FE MODEL AND APLI BS SOLID MODEL (FINALISED SPECIFICATIONS)

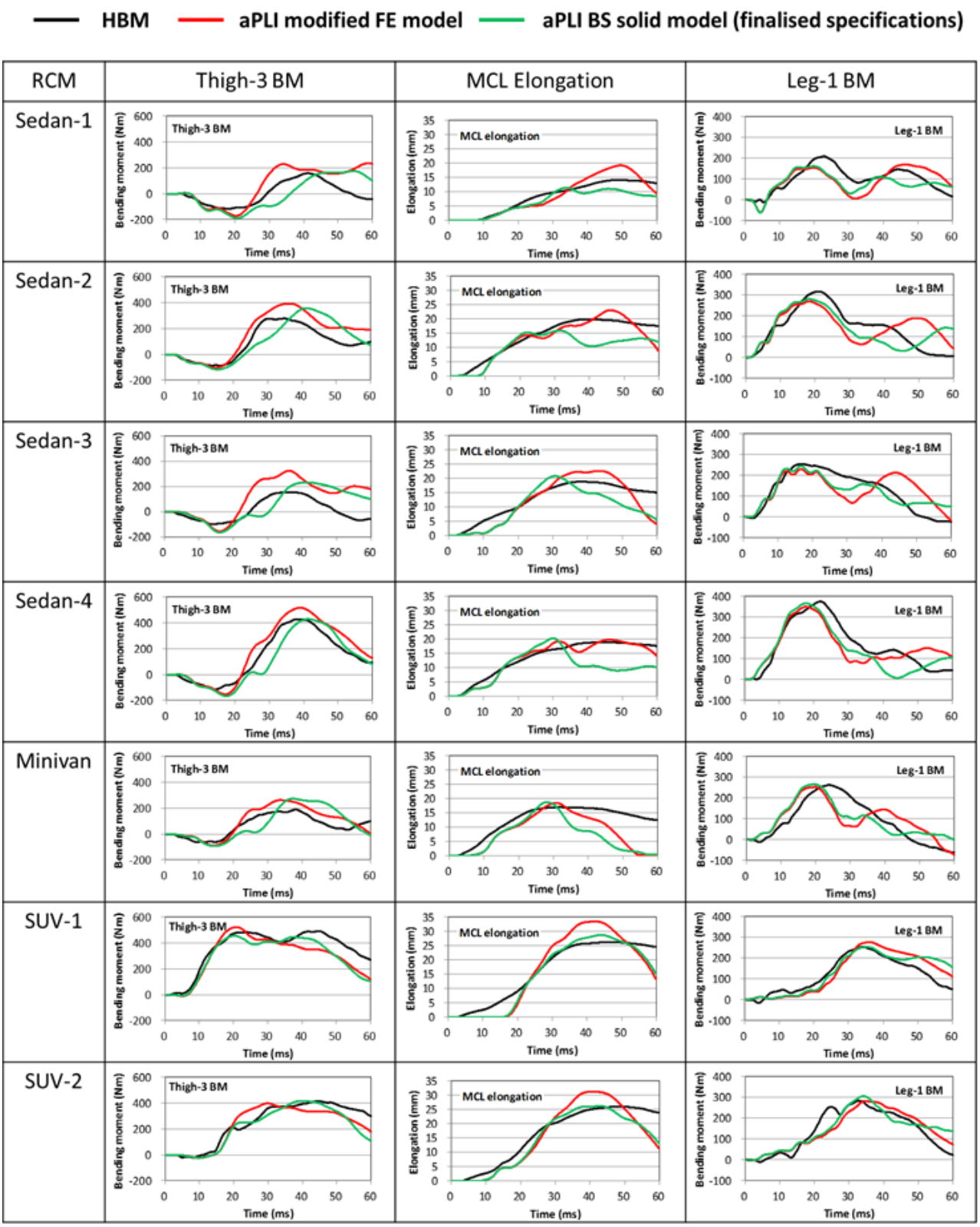

Fig. H1. Comparison of time history plots of Thigh-3 BM, MCL elongation and Leg-1 BM among HBM, aPLI modified FE model and aPLI BS solid model (finalised specifications) in seven-RCM impacts.

APPENDIX I: TIME HISTORY PLOTS OF APLI BS HARDWARE UNIT AND APLI BS SOLID MODEL (FINALISED SPECIFICATIONS)

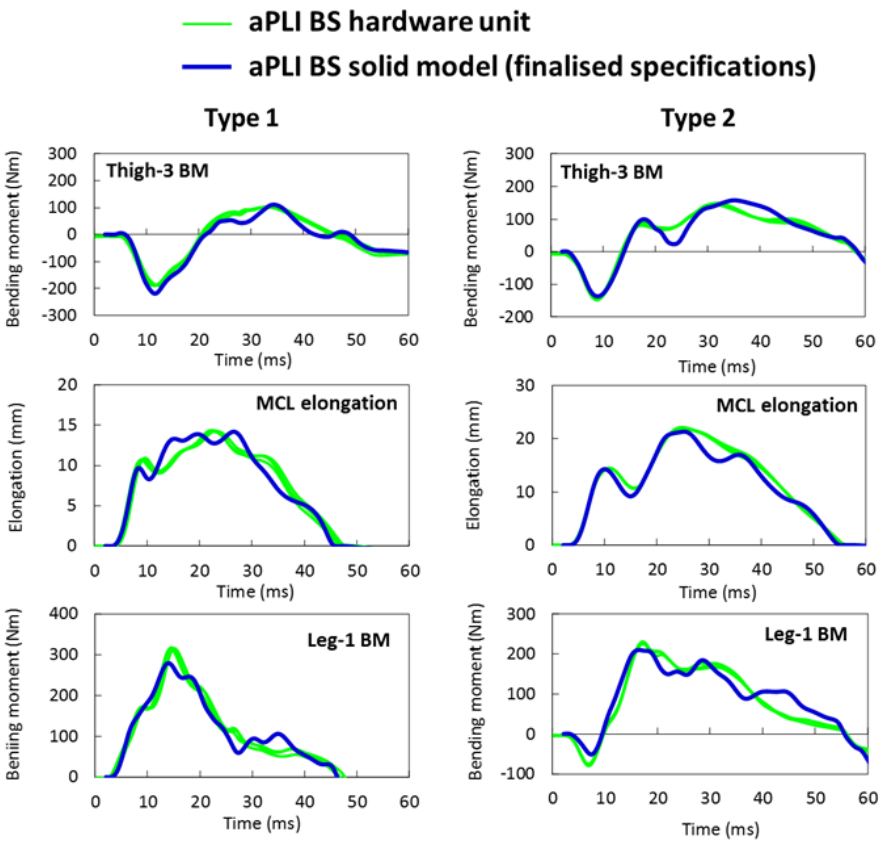

Fig. I1. Comparison of time history plots of Thigh-3 BM, MCL elongation and Leg-1 BM between aPLI BS hardware unit and aPLI BS solid model (finalised specifications) in inverse Type 1 and 2 tests (n=3) and simulations.